Article | Received 31 January 2025; Accepted 30 April 2025; Published 19 May 2025
https://doi.org/10.55092/rse20250003

Energy production forecasting: an application of the Grey Markov chain model to data from Italy

Guglielmo D'Amico[1], Riccardo De Blasis[2] and Veronica Vigna[2,*]

[1] Department of Economics, "G. d'Annunzio" University of Chieti-Pescara, Pescara, Italy

[2] Department of Management, Marche Polytechnic University, Ancona, Italy

* Correspondence author; E-mail: v.vigna@staff.univpm.it.

Highlights:

- Enhanced the $GM(1,N)$ model using Markov chains for residual correction.
- Improved forecasting for renewable and non-renewable energy production.
- Validated model performance using Italian energy data from 2004–2023.
- Addressed dynamic interactions between variables in energy systems.
- Supports strategic planning for Italy's sustainable energy transition.

Abstract: The multivariate Grey model ($GM(1,N)$) is a widely utilized forecasting tool within Grey models, capable of incorporating multiple variables. However, this model may present limitations in accuracy due to the structural differences between the Grey differential equations employed for parameter estimation and the whitening equation used for prediction. To overcome these issues, we propose an improvement to the $GM(1,N)$ model by adjusting the residuals with a multivariate Markov chain. Thus, we develop the $GMCM(1,N)$ model, which integrates the Mixture Transition Distribution (MTD) approach to model the interdependencies among residuals in multiple series. The use of the MTD model allows us to reduce the errors in parameter estimation in the Markov multivariate model. The proposed method improves the accuracy of representing dynamic interactions among variables and significantly increases the overall accuracy of the prediction. Finally, we apply the $GMCM(1,N)$ model to the energy sector, a domain where multivariate Grey-Markov approaches are still scarcely explored. We test the performance of the model using historical data for both renewable and non-renewable energy production for Italy. Furthermore, accurate energy production forecasts could support strategic energy planning and policy development, highlighting the practical relevance and potential applications of the improved model within the Italian energy sector.

Keywords: Grey model; Markov chain; multivariate; energy

1. Introduction

Accurate forecasting of energy production is crucial for strategic energy planning and policy development. Ensuring precise predictions helps optimize resource allocation, improve energy security, and support the country's transition to a more sustainable energy mix.

Various methodological approaches are used to effectively predict energy variables. Econometric models, such as vector autoregression (VAR) [1–4], autoregressive integrated moving average (ARIMA) [5,6], and cointegration models [7,8], are widely used due to their strong statistical foundations and the ability to capture temporal dependencies in the data. These approaches leverage historical data to identify patterns and relationships among different economic variables, providing valuable insights for short- and long-term forecasting. In addition to econometric methods, machine learning techniques such as Artificial Neural Networks (ANN) [9,10], Support Vector Machines (SVM) [11,12], and Random Forests [13,14] have gained popularity for their ability to handle large datasets and model complex nonlinear relationships.

Grey Systems Theory (GST), developed by Julong Deng [15], offers a systematic framework for managing uncertainty and limited data in complex systems. Particularly valuable in applied sciences and engineering, GST enables researchers to model and predict system behavior using incomplete or fragmented datasets. By extracting meaningful insights from minimal information, GST extends predictive capabilities beyond traditional modeling techniques, addressing challenges such as data scarcity and unreliability that are prevalent in many scientific contexts [16]. In particular, GST is applied in numerous fields, such as optimal resource management for energy and environmental emissions [17–19], sustainability policies in companies [20], social sciences [21], engineering disciplines [22], traffic and transportation [23], and the efficiency of supply chain management [24].

Within the framework of GST, the Grey model, often denoted as $GM(M,N)$, involves M-order partial differential equations with N variables, providing a structured approach to abstract the underlying mechanisms of a given system. Grey modeling operates on the premise that the complexities of a process can be simplified and represented by a suitable differential equation that captures the key dynamics. Parameter estimation within this framework is typically performed by analyzing relevant historical data. In particular, this modeling approach stands out due to its ability to generate forecasts using as few as four data points [25]. Among the commonly used Grey models, first-order $GM(1,1)$ is particularly prominent in the literature [18,26], as well as its multivariate counterpart $GM(1,N)$, which can incorporate the interconnections between multiple variables for more accurate forecasting [27–29].

However, since its inception, GST has seen substantial methodological evolution. Advances in GST have encouraged the development of novel techniques that improve the ability to work with incomplete, ambiguous, or inadequate datasets [30]. For example, Tien [31,32] proposed a convolution-based model to address known limitations in the solution structure of $GM(1,N)$, offering improved accuracy by integrating a Grey control parameter and modeling the system response through convolution integrals. In addition, in some real-world applications, data are often influenced by a range of unpredictable factors, resulting in data sequences that are volatile and exhibit high variability. Although the $GM(1,1)$ and $GM(1,N)$ models are effective in forecasting small datasets, they struggle when applied to data with significant

fluctuations [33]. To enhance their predictive accuracy in such cases, the Grey Markov chain model ($GMCM(1,1)$) was introduced [34–36]. This model corrects the residual errors produced by $GM(1,1)$ by incorporating Markov chains. The $GMCM(1,1)$ model combines single-variable first-order Grey forecasting with Markov chain adjustments to effectively capture the randomness and fluctuations present in the data [37–39]. This last approach has been successfully applied to small datasets characterized by randomness and volatility [40–42]. The fundamental concept behind $GMCM(1,1)$ is to categorize the residuals of $GM(1,1)$ into discrete states, then use Markov transition probability matrices to understand the statistical behavior of these residuals, ultimately refining the original forecast to achieve greater accuracy. Nevertheless, apart from [43], who propose a univariate Markov correction to a $GM(1,N)$ model, to our knowledge, an extension of the Grey Markov chain model to a full multivariate setting, thus including a multivariate Markov correction, is lacking in the literature.

Therefore, we propose a modification of the univariate Grey Markov chain model $GMCM(1,1)$ to model multiple time series, thus introducing the $GMCM(1,N)$ model. By extending the existing framework, our approach aims to capture a broader range of dynamics and improve the model's adaptability to complex multivariate datasets. This modification is designed to address existing limitations by enhancing the generalization capacity of the Grey Markov Chain model, ultimately leading to more accurate and robust predictions. The novelty of the proposed $GMCM(1,N)$ model lies in its explicit handling of multivariate dependencies among residual errors through the use of the Mixture Transition Distribution (MTD) model [44–46]. The MTD approach allows us to model multivariate time series through multiple convex linear combinations of transition probability matrices, thus reducing the number of parameters to estimate. The weights of these combinations measure the influence of one residual series on another. Moreover, unlike the univariate $GMCM(1,1)$, the $GMCM(1,N)$ explicitly models the dynamic interactions among residual errors of multiple series, effectively capturing interdependencies and significantly improving prediction accuracy in complex systems. Second, we demonstrate the utility of this extended model by applying it in the energy sector. This application not only validates the model's performance in a specific domain but also highlights its potential for making strategic energy planning more reliable, particularly in the integration of renewable and non-renewable energy sources.

The significance of this topic lies in its role in strategic planning and policymaking, which are crucial to achieving environmental targets and ensuring energy security. In addition, forecasting the energy mix is vital for identifying both the challenges and opportunities involved in the energy transition. For example, it provides information on how Italy can diversify its energy portfolio to reduce its dependency on imported fossil fuels, thus boosting energy security. In addition, it helps to highlight economic opportunities linked to the energy transition, such as technological innovations and the creation of jobs in the renewable energy sector [47].

Italy was chosen for this study because of its unique role in the European Union and the challenges it faces in aligning its energy strategy with EU targets. As an EU member, forecasting Italy's energy mix is essential for meeting ambitious goals related to reducing greenhouse gas emissions and increasing renewable energy by 2030 and beyond. The importance of Italy as a case study is due to its position as a mature industrial economy, uniquely sensitive to energy shifts due to its geographical characteristics

and lack of nuclear power facilities. These attributes play a significant role in shaping national energy strategies and influencing broader European energy policies. Predicting future energy composition helps prepare the necessary infrastructure, such as improving grid systems and energy storage solutions, to support a greater integration of intermittent renewable energy sources such as wind and solar energy [48].

The paper is organized as follows. In Section 2, we present the model. Specifically, in Subsection 2.1, we illustrate the steps of the Grey model $GM(1,N)$, in Subsection 2.2, we explain how to apply the multivariate Markov chain for error adjustment and obtain the prediction $GMCM(1,N)$. Subsequently, in Section 3, we present our case study on forecasting the consumption of primary energy from various sources for Italy. In addition, we validate the accuracy of our forecasts and the robustness of our models through a sensitivity analysis. In Section 4, the conclusions of our work are given.

2. Methods

The $GM(1,N)$ model leverages a first-order differential equation to characterize the target variable for forecasting, serving as a fundamental method in Grey system prediction. Furthermore, merging the Grey system with Markov chain theory offers enhanced statistical evaluations for datasets exhibiting pronounced variability. Notably, the Grey Markov Model operates without stringent assumptions regarding inter-variable relationships. However, to achieve reliable results, its deterministic component should effectively capture the underlying data trend, while the Markov chain component should refine these deterministic projections.

2.1. Grey $GM(1,N)$ model

While the comprehensive technical details and step-by-step procedures of the Grey model are extensively documented in the Appendix, this section highlights the essential components and the overarching framework employed in our analysis. This approach allows us to leverage existing theoretical foundations while focusing on the application and enhancement of the model within the context of Italian energy production data.

The forecasting process begins by organizing the time series data of each variable, which allows the model to capture trends and patterns over time. Suppose the panel data are:

$$X_i^{(0)} = \{x_i^{(0)}(1), x_i^{(0)}(2), \ldots, x_i^{(0)}(T)\}, \quad i = 1,2,\ldots,T,$$

where i stands for the variable and T is the number of observations. Subsequently, the model generates accumulated sequences to smooth out fluctuations and better reveal the underlying trends. These accumulated sequences are essential to establish a more stable prediction basis, and they are obtained through a summation operator defined in Equation (4) of Appendix A.

Then we define the background values $z_i^{(1)}(t)$ as weighted averages of consecutive cumulative data points. These values help to construct the differential equations that form the backbone of the forecasting mechanism. By solving these equations, the model estimates the future values of the target variable based on the historical data of both the target and the influencing variables. According to the steps shown in the

Appendix A, the equation used for the prediction of the accumulated value is

$$\hat{x}_1^{(1)}(t) = e^{-a\cdot(t-1)}\left[x_1^{(1)}(1) - \frac{1}{a}\left(\sum_{i=2}^{N} b_i x_i^{(1)}(t+1) + b_{N+1}\right)\right] + \frac{1}{a}\left(\sum_{i=2}^{N} b_i x_i^{(1)}(t+1) + b_{N+1}\right),$$

where a is called the system development coefficient and b_i is called the driver coefficient. These parameters are estimated according to the ordinary least squares procedure outlined in Appendix A. Finally, by subtracting consecutive values $\hat{x}^{(0)}(t) = \hat{x}^{(1)}(t) - \hat{x}^{(1)}(t-1)$, it is possible to compute the predicted values of the model.

2.2. *GMCM*$(1,N)$ *prediction*

Data observations frequently exhibit fluctuations due to various random factors, which complicates the generation of precise forecasts with the Grey model. To address this issue, we incorporate a Markov chain model to refine residual errors. Specifically, the Grey Markov chain model combines the Grey forecasting technique of $GM(1,N)$ with a Markov chain framework into a $GMCM(1,N)$ model to correct for these residual discrepancies. This approach involves categorizing the residuals from $GM(1,N)$ into distinct states, followed by the computation of Markov transition probability matrices to capture the statistical properties of these residuals and ultimately applying the adjustments derived from these matrices. This sequence improves the forecasting accuracy of the original Grey model.

For each time t, the $GM(1,N)$ model applied to each "pivot" series produces a vector of predictions $(\hat{x}_1^{(0)}(t), \hat{x}_2^{(0)}(t), \ldots, \hat{x}_N^{(0)}(t))$ to compare with the "real" data $(x_1^{(0)}(t), x_2^{(0)}(t), \ldots, x_N^{(0)}(t))$. The discrepancies between the predicted and observed data produce the residual vector $(\varepsilon_1(t), \varepsilon_2(t), \ldots, \varepsilon_N(t))$. Following [49], we compute the residual values of the i-th variable, using absolute errors, $\varepsilon_i = \hat{x}_i^{(0)}(t) - x_i^{(0)}(t)$. Instead, other authors employ relative errors [42,50].

Then we discretize each residual series into m quantiles, each quantile representing a state of the Markov chain. Let $S_i(t)$ denote the series of discretized residuals for each variable i. We then assume that each series $S_i(t)$ is governed by a multivariate Markov chain (MMC). Intuitively, this implies that the future state of any given variable depends not only on its own most recent state but also on the current states of all other variables in the system. For example, the probability of transitioning to state v at time $t+1$ for series 1 is influenced by its current state $S_1(t) = u_1(t)$, as well as the current states of all other variables $S_2(t) = u_2(t), \ldots, S_N(t) = u_N(t)$. This framework acknowledges the interconnected nature of the system, where the behavior of one variable's residuals is inherently linked to the states of the residuals of other variables.

By considering the latest information from all relevant variables, the MMC framework captures the dynamic interactions and dependencies that drive the system's evolution. The formal mathematical representation of the MMC is

$$\begin{aligned}\Pr\left[S_1(t+1) = v \mid\right. & \left(S_1(t) = u_1(t), S_1(t-1) = u_1(t-1), \ldots, S_1(1) = u_1(1)\right), \ldots, \\ & \left.\left(S_N(t) = u_N(t), S_N(t-1) = u_N(t-1), \ldots, S_N(1) = u_N(1)\right)\right] \\ & = \Pr\left[S_1(t+1) = v \mid S_1(t) = u_1(t), \ldots, S_N(t) = u_N(t)\right].\end{aligned}$$

A similar relationship holds for all other variables from 2 to N.

When the number of states m of the MMC and the number of series N increase significantly, the number of independent parameters grows exponentially. To address this issue, following [46], we employ the Mixture Transition Distribution (MTD) model initially proposed by [44,45] to approximate high-order Markov chains. Specifically, the MTD model approximates a high-dimensional Markov chain as follows

$$\mathbf{A}_\alpha(t+1) = \sum_{\beta=1}^{N} \mathbf{A}_\beta(t) \cdot \lambda_{\beta,\alpha} \cdot \mathbf{P}^{(\beta,\alpha)}, \tag{1}$$

where $\mathbf{A}_\alpha(t) := (A_{\alpha;1},\ldots,A_{\alpha;m})$ with $A_{\alpha;u}(t) := Pr[S_\alpha(t) = u]$, and the matrices $\mathbf{P}^{(\beta,\alpha)}$ contain the transition probabilities from state u in series β to state v in series α.

The application of the MTD model in (1) requires the estimation of the parameters $\lambda_{\beta,\alpha}$ for each series. Therefore, we obtain a matrix of weights,

$$\mathbf{\Lambda} = \begin{pmatrix} \lambda_{11} & \lambda_{12} & \ldots & \lambda_{1N} \\ \lambda_{21} & \lambda_{22} & \ldots & \lambda_{2N} \\ \vdots & \vdots & \ddots & \vdots \\ \lambda_{N1} & \lambda_{N2} & \ldots & \lambda_{NN} \end{pmatrix},$$

which quantify the relative influence of the residual state of one variable β on another variable α.

The discretized series of residuals $S_i(t)$ can be identified as

$$S_i(t) = e_{i;u_i}, \quad i = i,\ldots,N, u_i = 1,\ldots,m,$$

where $e_{i;u_1}$ identifies the state through the unit vector, e.g., $\mathbf{e}_{i;1} = (1,0,0,\ldots,0)$, $\mathbf{e}_{i;2} = (0,1,0,\ldots,0)$, and so on.

Therefore, by Equation (1) and knowing the states of all series at time t, we can predict the state of time series α as follows

$$P\left[S_\alpha(t+1) = e_{\alpha;v} | S_1(t) = e_{1;u_1}, S_2(t) = e_{2;u_2}, \ldots, S_N(t) = e_{N;u_N}\right] = \sum_{\beta=1}^{N} e_{\beta;u_\beta} \cdot \lambda_{\beta,\alpha} \cdot p_{u_\beta,v}^{(\beta,\alpha)}. \tag{2}$$

However, to obtain the exact prediction for the specific series α, we need to identify a representative value $r_{i;v}$ for each quantile v of the discretization, which we can compute as a simple average. Therefore, the adjustment will be

$$\hat{\varepsilon}_\alpha = \sum_{j=1}^{m} \sum_{\beta=1}^{N} e_{\beta;u_\beta} \cdot \lambda_{\beta,\alpha} \cdot p_{u_\beta,v}^{(\beta,\alpha)} \cdot r_{\alpha;v}. \tag{3}$$

The presented formula calculates a weighted average that accounts for the interconnections between variables through the transition probabilities and the MTD weights.

Finally, we get the adjusted prediction in the following way

$$\hat{\hat{x}}_1^{(1)}(t) = \hat{x}_1^{(1)}(t) + \hat{\varepsilon}_\alpha.$$

If we need to apply the forecast from t to $t+k$, instead of $p_{u_\beta,v}^{(\beta,\alpha)}$, which is the one-step matrix, we should use the corresponding elements of $\left(\mathbf{P}^{(\beta,\alpha)}\right)^k$, which is the k-step transition matrix.

3. Results

We apply the $GM(1,N)$ model with residual correction through Markov chains to historical data on primary energy consumption in Italy, sourced from the Our World in Data website (https://ourworldindata.org). Table 1 provides an overview of the annual consumption in terawatt hours (TWh) for various sources of primary energy in Italy from 2004 to 2023. The table includes data for biofuels, coal, gas, hydro, oil, solar, and wind energy, highlighting significant shifts in Italy's energy profile over the last two decades. Focusing on these 20 years allows for a detailed analysis of recent trends and patterns in Italian energy consumption, offering a relevant foundation for the predictive model, which aims to improve the accuracy of forecasts for renewable and non-renewable energy production.

Table 1. Italian annual primary energy consumption by source from 2004 to 2023 (TWh).

Year	Biofuel	Coal	Gas	Hydro	Oil	Solar	Wind
2004	2.754	193.013	773.418	122.003	1072.420	0.084	5.322
2005	1.933	191.534	827.695	103.275	1039.467	0.089	6.709
2006	2.178	193.911	810.588	105.263	1038.177	0.100	8.454
2007	1.977	189.848	814.561	92.788	1005.712	0.110	11.407
2008	7.983	183.701	808.515	116.963	946.612	0.542	13.660
2009	12.885	143.823	743.176	137.228	875.992	1.891	18.273
2010	15.864	159.028	791.499	141.879	853.391	5.289	25.330
2011	15.672	178.270	742.161	126.410	828.881	29.782	27.190
2012	17.494	182.733	713.566	114.819	772.214	51.718	36.761
2013	14.687	157.403	667.404	143.831	706.480	58.838	40.601
2014	12.546	153.447	589.716	158.604	671.279	60.430	41.119
2015	15.486	143.395	643.154	122.631	710.444	61.783	39.974
2016	15.401	127.732	675.458	113.592	704.790	59.174	47.353
2017	15.610	111.904	715.788	96.335	713.695	64.876	47.216
2018	15.979	102.567	692.141	129.177	730.328	59.936	46.873
2019	9.359	77.534	707.906	122.194	709.052	62.443	53.252
2020	13.227	59.253	676.252	125.100	585.492	65.504	49.273
2021	13.822	65.182	723.737	118.766	651.104	65.519	54.760
2022	12.353	86.385	651.990	74.036	695.903	73.317	53.431
2023	14.190	60.218	585.976	101.110	686.874	81.118	61.124

Primary energy represents the total quantity of energy available from primary sources, that is, those found in nature without any conversion, such as coal, oil, natural gas, wind, solar, and hydroelectric power. In other words, primary energy includes energy extracted directly from the environment without any initial transformation. It is distinct from secondary energy, which is the result of converting primary

energy into forms usable by humans, such as electricity or heat. In the Italian context, monitoring primary energy consumption is particularly relevant for understanding the dynamics of dependence on imported energy sources and evaluating the effectiveness of transition policies toward renewable energy sources.

The proposed model uses these data to identify and forecast trends, considering the unique characteristics of the Italian energy system. We chose Italy as a case study due to its specific challenges in aligning its energy strategy with the goals of the European Union to reduce greenhouse gas emissions and increase renewable energy by 2030. Italy's energy decisions have significant national and regional impacts as one of the largest European economies with a substantial and growing industrial sector.

The data reveal several notable trends over the last two decades, highlighting significant changes in Italy's energy profile and reflecting its ongoing transition toward a more sustainable energy mix.

Coal consumption experienced a marked decline during this period, starting at 193.013 TWh in 2004 and dropping to 60.218 TWh in 2023. This substantial reduction aligns with Italy's strategic efforts to decrease coal dependence in favor of cleaner energy sources, consistent with the policies of the European Union to reduce greenhouse gas emissions. Natural gas, while remaining a dominant energy source, showed notable fluctuations. Initially at 773.418 TWh in 2004, gas consumption peaked at 827.695 TWh in 2005 but gradually declined toward 2023, ending at 585.976 TWh. This decrease may suggest a shift in reliance on natural gas, potentially influenced by the increased adoption of renewable energy sources. Oil consumption followed a similar downward trend, falling from 1072.420 TWh in 2004 to 686.874 TWh in 2023. Although oil still represents a significant part of the energy mix, its decline indicates Italy's gradual transition away from traditional fossil fuels, driven in part by rising oil prices and environmental policies. Hydropower contributed a stable but variable amount of energy, averaging around 120 TWh annually, with peaks such as 158.604 TWh in 2014. This variability is likely due to seasonal rainfall patterns and hydrological conditions, underscoring hydro's role as a key, yet fluctuating renewable resource. Solar and wind energy, on the contrary, exhibited substantial growth, demonstrating Italy's commitment to expand its renewable infrastructure. Solar energy, almost negligible in 2004 at 0.084 TWh, increased exponentially to 81.118 TWh in 2023. Wind energy followed a similar upward trend, growing from 5.322 TWh in 2004 to 61.124 TWh in 2023. This remarkable increase in both solar and wind energy highlights the rapid integration of renewables into Italy's energy portfolio. Biofuel, though a less prominent energy source than solar or wind, increased from 2.754 TWh in 2004 to 14.190 TWh in 2023, adding another renewable element to the Italian energy mix. Together, these trends reflect Italy's transition from fossil fuels, particularly coal and oil, to renewables, in line with its goals to diversify the energy mix and meet EU goals for reducing carbon emissions and expanding sustainable energy. It should be noted that nuclear energy is not reported in Table 1, as its contribution to Italy's primary energy mix has remained zero throughout the period from 2004 to 2023. This absence is due to Italy's long-standing policy against nuclear energy. Following a national referendum in 1987, shortly after the Chernobyl disaster, Italy decided to shut down its existing nuclear power plants and abandon further nuclear development. Subsequent referendums in 2011, amid renewed discussions on nuclear energy, reaffirmed this decision, with a majority of the Italian population voting against the revival of nuclear power. As a result, Italy is one of the few major European economies without active nuclear power generation, which influences its

reliance on other sources, especially imports, and places additional emphasis on expanding renewable energy as part of its commitment to sustainability and energy independence.

To illustrate the application of the $GM(1,N)$ model with Markov chain residual correction, we show each step of the methodology using biofuel data as an example.

The initial step involves data preparation, where we extract the primary energy consumption data for biofuel in terawatt hours (TWh) from the dataset and organize them into a time series format:

$$\begin{aligned} X^{(0)}_{\text{biofuel}} = (&2.754, 1.933, 2.178, 1.977, 7.983, 12.885, 15.864, 15.672, \\ &17.494, 14.687, 12.546, 15.486, 15.401, 15.610, 15.979, 9.359, \\ &13.227, 13.822, 12.353, 14.190)^T. \end{aligned}$$

Next, we perform the first-order accumulation operation according to Equation (4) of Appendix A. This step involves accumulating the original biofuel data series to produce a smoothed sequence, reducing noise and revealing underlying trends. We denote the accumulated series as

$$\begin{aligned} X^{(1)}_{\text{biofuel}} = (&2.754, 4.687, 6.865, 8.842, 16.825, 29.710, 45.574, 61.246, \\ &78.740, 93.427, 105.973, 121.459, 136.860, 152.470, 168.449, 177.808, \\ &191.035, 204.857, 217.210, 231.400)^T, \end{aligned}$$

which becomes the basis for constructing the Grey differential equations used in the forecasting model.

With the accumulated series in place, we proceed to the parameter estimation phase. Here, we estimate the parameters of the model $GM(1,N)$ by analyzing the relationships between biofuel data and other energy sources. These parameters include the system development coefficient, a and the driving coefficients, b_i, where $i = 2,\ldots,N+1$, for the influence of other energy variables on biofuel. The parameter estimation process involves solving Equation (7), which leads to the following estimates

$$\hat{B} = (-0.056, -0.027, -0.019, 0.010, 0.021, -0.068, 0.072, -4.179)^T,$$

In this notation, the first element, -0.056, represents the coefficient a, known as the system development coefficient. Its small negative value indicates a slow decay in the system's response over time, reflecting a decreasing trend in the accumulated series, which is consistent with the energy consumption models stabilizing over time. The subsequent elements, from -0.027 to 0.072, represent the coefficients b_i, where $i = 2,\ldots,N$ corresponds to the influence of each variable on the biofuel system. Positive values, such as $b_5 = 0.021$ and $b_7 = 0.072$, suggest a direct relationship, indicating that these variables contribute positively to biofuel trends. In contrast, negative values, such as $b_6 = -0.068$, indicate an inverse relationship, where these variables suppress biofuel trends. The final element, -4.179, represents b_{N+1}, an intercept term that accounts for systematic offsets, capturing baseline factors not directly attributed to the other variables, thereby ensuring that the model's predictions align more closely with observed data.

Once the parameters are estimated, we then construct the whitening differential equation for biofuel,

which translates the accumulated data into a differential form to capture the trend. This equation forms the predictive component of the Grey model, allowing us to calculate the forecast values for biofuel consumption. Figure 1 shows the comparison between the observed and predicted primary energy consumption in TWh. The solid blue line with circular markers represents the observed biofuel values in terawatt hours (TWh), while the dashed orange line with cross markers shows the predicted values obtained using the $GM(1,N)$ model. The chart highlights the model's effectiveness in capturing general trends, with some deviations visible in years with rapid changes or fluctuations. This comparison provides insight into the predictive performance of the model and its ability to adapt to variations in biofuel consumption over time.

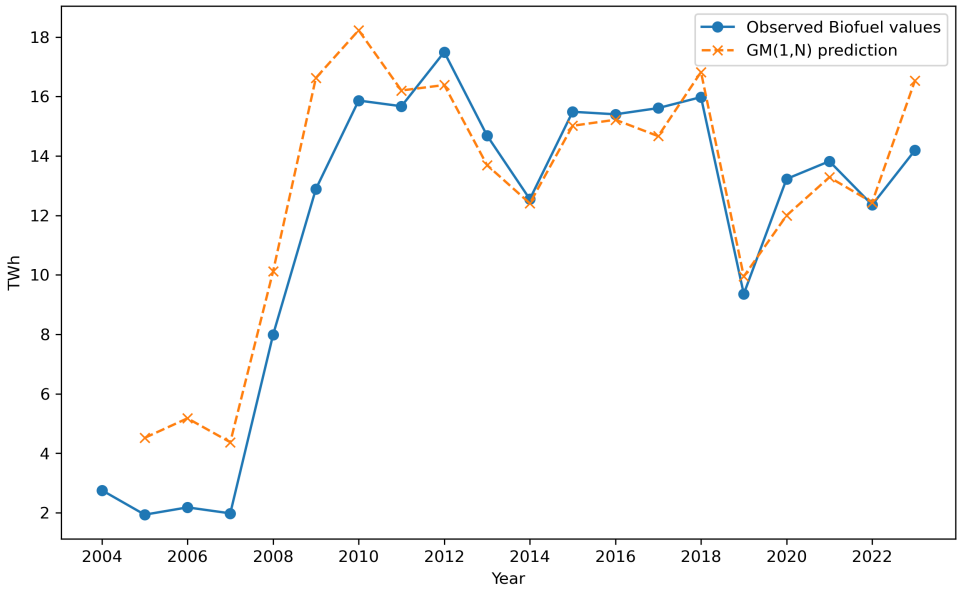

Figure 1. Comparison between observed and predicted biofuel energy consumption in Italy from 2004 to 2023.

After generating the initial forecasts, we apply the Markov chain residual correction to enhance the accuracy of the model. This step addresses the inherent variability and potential errors in the initial forecast by analyzing the residuals, or differences, between the model predictions and the observed biofuel data. The residuals related to biofuel are as follows

$$\boldsymbol{\varepsilon}_{biofuel} = (2.584, 2.996, 2.392, 2.132, 3.737, 2.364, 0.530, -1.109, -0.995, -0.141, \\ -0.471, -0.184, -0.943, 0.842, 0.587, -1.231, -0.539, 0.086, 2.344)^T.$$

Then these residuals are categorized into discrete states. In our example, we categorize forecasting errors into three distinct states, which we define as "low error," "medium error," and "high error." This classification, shown in Figure 2, is achieved using a quantile-based method, which divides the error distribution into three parts based on the magnitude.

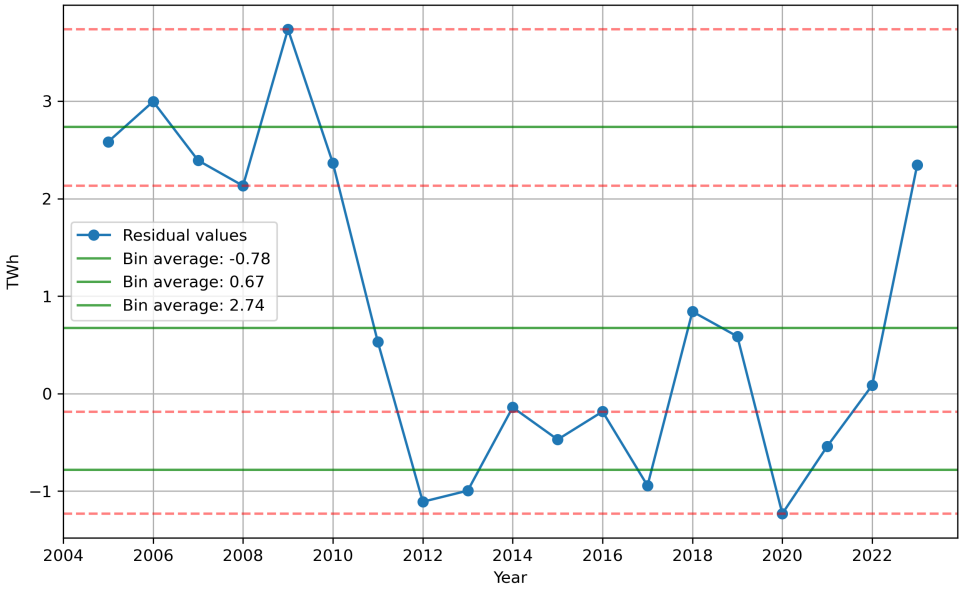

Figure 2. Residual values for biofuel forecasting errors from 2005 to 2023, divided into three quantile-based states.

The blue line with circular markers represents the residual values in terawatt hours (TWh), showing the differences between the observed and predicted biofuel values. The green horizontal lines indicate the average residual values for each quantile-based bin: -0.78 TWh for low residuals, 0.67 TWh for medium residuals, and 2.74 TWh for high residuals. Red dashed lines highlight the quantile boundaries. This visualization illustrates the variability of forecasting residuals and the categorization into distinct states for refined Markov chain adjustments based on error magnitude. By grouping the errors into these three states, we can apply targeted adjustments using the Markov chain approach, which refines the predictions based on the typical behavior within each error category.

After the discretization and based on the MTD model in (1), we can construct $N^2 = 49$ transition probability matrices $\mathbf{P}^{(\beta,\alpha)}$, where each matrix contains the transition probabilities from state u in series β to state v in series α. We estimate these transition probabilities by employing the maximum-likelihood estimator,

$$\hat{p}_{uv}^{(\beta,\alpha)} = \frac{n_{uv}^{(\beta,\alpha)}}{\sum_{v=1}^{m} n_{uv}^{(\beta,\alpha)}},$$

where $n_{uv}^{(\beta,\alpha)}$ is the occurrences of transitions from state u in series β to state v in series α.

In our case, fixing α as the biofuel series, we obtain seven 3×3 transition probability matrices for biofuel from all energy sources:

$$\mathbf{P}^{(\text{Biofuel,Biofuel})} = \begin{bmatrix} 0.571 & 0.429 & 0.000 \\ 0.500 & 0.167 & 0.333 \\ 0.000 & 0.400 & 0.600 \end{bmatrix} \quad \mathbf{P}^{(\text{Coal,Biofuel})} = \begin{bmatrix} 0.167 & 0.167 & 0.667 \\ 0.667 & 0.333 & 0.000 \\ 0.333 & 0.500 & 0.167 \end{bmatrix}$$

$$\mathbf{P}^{(\text{Gas,Biofuel})} = \begin{bmatrix} 0.333 & 0.333 & 0.333 \\ 0.333 & 0.333 & 0.333 \\ 0.500 & 0.333 & 0.167 \end{bmatrix} \quad \mathbf{P}^{(\text{Hydro,Biofuel})} = \begin{bmatrix} 0.500 & 0.333 & 0.167 \\ 0.333 & 0.667 & 0.000 \\ 0.333 & 0.000 & 0.667 \end{bmatrix}$$

$$\mathbf{P}^{(\text{Oil,Biofuel})} = \begin{bmatrix} 0.429 & 0.429 & 0.143 \\ 0.333 & 0.333 & 0.333 \\ 0.400 & 0.200 & 0.400 \end{bmatrix} \quad \mathbf{P}^{(\text{Solar,Biofuel})} = \begin{bmatrix} 0.500 & 0.167 & 0.333 \\ 0.167 & 0.500 & 0.333 \\ 0.500 & 0.333 & 0.167 \end{bmatrix}$$

$$\mathbf{P}^{(\text{Wind,Biofuel})} = \begin{bmatrix} 0.429 & 0.286 & 0.286 \\ 0.500 & 0.333 & 0.167 \\ 0.200 & 0.400 & 0.400 \end{bmatrix}$$

As an example, consider the transition probability matrix $P^{(\text{Wind,Biofuel})}$, which provides insight into how the residual state of the *Wind* variable at a given time influences the residual state of the *Biofuel* variable at the next time step. Each row of the matrix corresponds to a current residual state of *Wind*, while each column represents a possible subsequent state of *Biofuel*. If there were no influence of *Wind* residuals on *Biofuel*, the transition probabilities within each row would be uniformly distributed and all rows of the matrix would be identical. However, the fact that the rows in $P^{(\text{Wind,Biofuel})}$ are distinct indicates that the residual state of *Wind* affects the residual state of *Biofuel* at the next time step. This non-uniform distribution of probabilities highlights the dependency between these two variables, reinforcing the validity of using a multivariate Markov chain-based approach to model these interactions.

Subsequently, following [51,52], we estimate the parameters $\lambda_{\beta,\alpha}$, which act as scalar weights that integrate all the series, maximizing the log-likelihood function associated with the multivariate model as follows

$$\log L = \sum_{u_1,u_2,\ldots,u_N,v} n_{u_1,u_2,\ldots,u_N,v} \log P_{\alpha}^{MTD},$$

where $P_{\alpha}^{MTD} = \lambda_{1\alpha} P_{u_1,v}^{(1,\alpha)} + \cdots + \lambda_{N,\alpha} P_{u_N,v}^{(N,\alpha)}$ is the linear combination of the transition probabilities from states u_N of series N to state v of series α. The values $n_{u_1,u_2,\ldots,u_N,v}$ designate the number of observed transition combinations of the type $(u_1,u_2,\ldots,u_N)$ at time $t-1$ to state v of series α at time t. This maximization process is subject to the constraints $\sum_{\beta=1}^{N} \lambda_{\beta,\alpha} = 1$ and $\lambda_{\beta,\alpha} \geq 0$.

Table 2 presents the scalar weights that quantify the relative influence of the residual state of one variable (rows) on another variable (columns) in the next time step. These weights are critical for capturing the dynamic interactions between variables. For example, the influence of *Hydro* residuals on *Biofuel* residuals is 0.590. This high weight indicates that the residual state of *Hydro* significantly impacts the residual state of *Biofuel* in the following time step, highlighting a strong dependency. On the other hand, the influence of *Biofuel* residuals on *Hydro* is 0.502, showing that while *Biofuel* does influence *Hydro*, the dependency is slightly weaker compared to the reverse relationship. Another notable interaction is between *Coal* and *Wind*, where *Coal* residuals strongly influence *Wind* residuals with a weight of 0.759.

This indicates that the state of *Coal* plays a dominant role in determining the subsequent state of *Wind*. Similarly, *Wind* residuals moderately influence *Solar* residuals with a weight of 0.391, suggesting a less pronounced but still significant dependency. The non-uniform distribution of the weights across the table demonstrates that not all variables exert equal influence. Instead, the interactions are variable-specific and context-dependent, emphasizing the complex interdependencies in the system. This variability reinforces the suitability of using a multivariate Markov chain-based model, as it effectively accounts for these weighted relationships, leading to more accurate and reliable forecasts.

Table 2. $\lambda_{\beta,\alpha}$ parameters estimated by maximizing the log-likelihood function associated with the multivariate model.

	Biofuel	**Coal**	**Gas**	**Hydro**	**Oil**	**Solar**	**Wind**
Biofuel	0.181	0.211	0.000	0.502	0.079	0.000	0.000
Coal	0.230	0.743	0.154	0.000	0.000	0.176	0.759
Gas	0.000	0.000	0.328	0.000	0.000	0.000	0.000
Hydro	0.590	0.000	0.000	0.000	0.647	0.000	0.030
Oil	0.000	0.000	0.519	0.000	0.274	0.000	0.000
Solar	0.000	0.046	0.000	0.000	0.000	0.433	0.000
Wind	0.000	0.000	0.000	0.498	0.000	0.391	0.211

Finally, we compute the adjustments to the forecasted values using Equation (3) and we calculate the adjusted forecast for biofuel by incorporating those Markov chain corrections into the initial forecast, producing a refined prediction for biofuel consumption. Figure 3 shows these results.

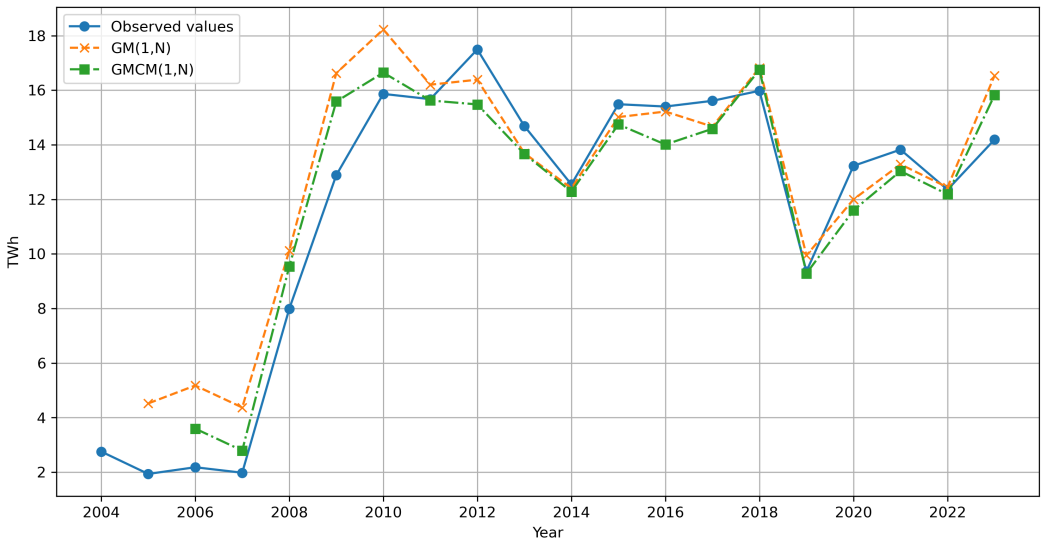

Figure 3. Comparison of observed and predicted biofuel energy consumption in Italy from 2004 to 2023 with *GM(1,N)* and *GMCM(1,N)*.

The blue line with circular markers represents the observed values in terawatt hours (TWh). The orange dashed line with cross markers indicates the predictions of the $GM(1,N)$ model, while the green

dash-dotted line with square markers shows the adjusted predictions of the $GMCM(1,N)$ model, which includes corrections based on Markov chain adjustments. This graph demonstrates the effectiveness of both models, with the $GMCM(1,N)$ model providing improved alignment with the observed data by incorporating corrections for residuals.

In addition, the accuracy indices for the biofuel forecasts reveal a clear improvement when using the $GMCM(1,N)$ model compared to the $GM(1,N)$ model. Table 3 provides a comparison of the mean absolute error (MAE), mean squared error (MSE), root mean squared error (RMSE), and coefficient R^2 for both models.

Table 3. Comparison of accuracy indices for biofuel between $GM(1,N)$ and $GMCM(1,N)$ Models.

Model	MAE	MSE	RMSE	R^2
$GM(1,N)$	1.379	3.026	1.740	0.872
$GMCM(1,N)$	1.046	1.569	1.253	0.918

In terms of MAE, the $GMCM(1,N)$ model achieves a lower value of 1.046 compared to 1.379 for the $GM(1,N)$ model, indicating a reduction in the magnitude of the average error. Similarly, the Mean Squared Error (MSE) is significantly reduced in the $GMCM(1,N)$ model, with a value of 1.569 compared to 3.026 in the $GM(1,N)$ model. This reduction in MSE also results in a RMSE of 1.253 in the $GMCM(1,N)$ model, down from 1.740 in the $GM(1,N)$ model, suggesting an overall decrease in residual variance. Furthermore, the coefficient R^2, which measures the proportion of variance in the observed data explained by the model, shows a noticeable increase in the $GMCM(1,N)$ model. The R^2 value increases from 0.872 in the $GM(1,N)$ model to 0.918 in the $GMCM(1,N)$ model. This higher value indicates that the $GMCM(1,N)$ model provides a better fit to the observed biofuel data, capturing more of the underlying variability.

Overall, the transition from $GM(1,N)$ to $GMCM(1,N)$ for biofuel results in improved forecasting accuracy across all metrics (MAE, MSE, RMSE, and R^2), highlighting the effectiveness of incorporating Markov chain corrections in reducing error and improving model fit. This improvement is especially relevant in contexts where precise prediction of biofuel consumption is essential for strategic energy planning and decision making. This step-by-step application demonstrates the capacity of the $GM(1,N)$ model to handle limited and variable data effectively, showcasing the adaptability and robustness of the model in predicting trends in energy consumption over time.

We repeated all previous steps for each energy source to generate accurate forecasts using the $GMCM(1,N)$ model. This process involved applying the same methodology to each energy source individually, ensuring consistency and allowing for a comparative analysis across different types of energy. The final results of the predictions obtained through the $GMCM(1,N)$ model for each energy source are summarized in Table 4.

We evaluated the accuracy of the forecasting models for each energy source using both the multivariate Grey model ($GM(1,N)$) and the extended version with multivariate Markov chain residual correction ($GMCM(1,N)$). Tables 5 and 6 summarize the accuracy indices and the coefficient of

determination for each model and energy source.

Table 4. $GMCM(1,N)$ prediction for each energy source in TWh.

Year	Biofuel	Coal	Gas	Hydro	Oil	Solar	Wind
2006	3.594	194.069	807.753	112.723	1035.548	2.356	6.788
2007	2.789	206.062	788.576	93.498	932.277	0.000	11.954
2008	9.536	202.057	802.923	118.472	891.770	7.339	14.383
2009	15.583	146.772	719.442	145.614	905.111	17.498	18.343
2010	16.644	189.792	727.490	139.102	784.162	10.931	29.376
2011	15.623	185.210	753.458	127.553	809.663	40.811	27.613
2012	15.479	204.680	724.554	115.553	734.010	58.470	37.327
2013	13.662	182.010	701.460	142.400	677.295	59.263	38.991
2014	12.282	166.243	570.872	154.427	681.516	53.336	39.430
2015	14.745	139.178	681.968	128.045	751.335	69.739	37.390
2016	14.008	141.728	619.136	110.257	676.519	56.976	48.900
2017	14.585	118.750	738.562	98.844	715.425	74.346	46.076
2018	16.748	104.482	687.526	134.623	795.352	61.564	45.659
2019	9.284	97.553	659.836	111.344	680.950	49.867	53.292
2020	11.597	84.754	768.750	122.994	591.440	81.812	44.466
2021	13.036	88.982	735.603	114.779	627.265	65.234	53.915
2022	12.183	82.102	592.885	71.176	718.348	64.006	54.570
2023	15.821	24.711	436.161	97.111	828.367	53.982	62.572

Table 5. $GM(1,N)$ accuracy indices.

	MAE	MSE	RMSE	R^2
Biofuel	1.379	3.026	1.740	0.872
Coal	14.205	387.745	19.691	0.822
Gas	39.534	2872.311	53.594	0.428
Hydro	5.522	45.006	6.709	0.882
Oil	39.895	2518.149	50.181	0.859
Solar	10.322	138.051	11.750	0.840
Wind	3.042	12.646	3.556	0.956

Table 6. $GMCM(1,N)$ accuracy indices.

	MAE	MSE	RMSE	R^2
Biofuel	1.046	1.569	1.253	0.918
Coal	15.045	334.159	18.280	0.841
Gas	37.846	2739.013	52.336	0.398
Hydro	3.824	22.023	4.693	0.944
Oil	37.991	2525.175	50.251	0.832
Solar	7.921	108.453	10.414	0.865
Wind	1.450	3.610	1.900	0.986

Both tables reveal that the $GMCM(1,N)$ model with multivariate Markov chain residual correction consistently improves the forecast accuracy in most energy sources compared to the traditional $GM(1,N)$ model. For example, in the case of biofuel, the MAE decreases from 1.379 to 1.046, and the MSE drops from 3.026 to 1.569, demonstrating a reduction in the magnitude and variance of the average error. We observe similar improvements for other energy sources, such as hydro and wind. For hydro, the MAE decreases from 5.522 to 3.824, and increases significantly from 0.882 to 0.944, illustrating the effectiveness of the residual correction in capturing the variability. Wind energy also benefits from the $GMCM(1,N)$ model, with a higher value of 0.986 compared to 0.956 in the $GM(1,N)$ model, suggesting a more accurate alignment with observed values. However, for energy sources such as gas, the improvement is less pronounced. Although the $GMCM(1,N)$ model slightly reduces MAE and MSE, the value decreases slightly from 0.428 to 0.398, indicating that further refinement may be needed for more volatile energy sources. Overall, the $GMCM(1,N)$ model demonstrates a substantial improvement in forecast accuracy for most energy sources, confirming the value of incorporating the multivariate Markov chain residual correction to enhance the predictive power of the traditional $GM(1,N)$ model.

4. Conclusion

In this study, we presented an enhanced forecasting model for energy production using Italian data by integrating the multivariate Grey model $GM(1,N)$ with a Markov chain correction mechanism, referred to as $GMCM(1,N)$. This approach addresses the inherent limitations of the traditional $GM(1,N)$ model, particularly in managing high variability and residual errors in the data, by applying Markov chains to categorize and adjust residuals. The results show that $GMCM(1,N)$ significantly improves the accuracy of the energy forecasts, as indicated by lower mean absolute error (MAE), mean squared error (MSE), root mean squared error (RMSE) and higher R^2 values. The accuracy improvements underscore the model's potential as a robust tool to forecast energy production in scenarios where data variability poses a challenge.

By applying the $GMCM(1,N)$ model to energy data from Italy, we validated its effectiveness in a real-world context. The proposed framework offers a reliable forecasting tool that may help policy makers and energy planners in achieving strategic energy goals. In fact, Italy's unique position in the EU and its commitment to transitioning to a more sustainable energy mix make accurate forecasts critical. This model not only aligns with Italy's objectives to reduce dependency on non-renewable sources, but also improves the reliability of projections for renewable energy integration.

Future work could explore the extension of this model to incorporate additional variables or to be applied in other regional or national contexts to further validate its flexibility and accuracy. The incorporation of additional datasets could also improve the model's adaptability, potentially offering more precise insights into renewable energy trends and helping to guide investments and policy in sustainable energy.

Despite its contributions, the present study has some limitations that suggest possible directions for future work. First, the model assumes fixed transition probabilities and discretized residual states; future research may investigate adaptive or non-homogeneous Markov structures. Second, the relatively

small size of the dataset motivated us to focus on Grey models, which are particularly suitable for data-scarce environments, and to avoid methods such as ARIMA that require larger and stationary time series. Third, the deterministic core of our model is based on the standard $GM(1,N)$; we deliberately chose not to compare with other deterministic Grey models (e.g., $GMC(1,N)$, DGM) to isolate and evaluate the specific contribution of the proposed multivariate stochastic correction mechanism. As a possible extension, the proposed correction strategy could be combined with more advanced deterministic models such as convolution-based Grey models ($GMC(1,N)$), Grey models with delay structures, or with adaptive parameters. These extensions could further improve forecast accuracy and flexibility, especially in contexts with evolving dynamics or larger variable sets.

Overall, the $GMCM(1,N)$ model presents a valuable contribution to the energy forecasting literature, providing a methodology capable of balancing precision with the complexities inherent in multivariate energy datasets.

Acknowledgments

The authors acknowledge the financial support from the European Union - NextGenerationEU program MUR PRIN 2022 n. 2022ETEHRM “Stochastic models and techniques for the management of wind farms and power systems” by the Italian Ministero dell’Universitá e della Ricerca. Riccardo De Blasis is a member of the Gruppo Nazionale Calcolo Scientifico-Istituto Nazionale di Alta Matematica (GNCS-INdAM).

Author’s contribution

Conceptualization: G.D.; methodology: G.D. and R.D.B.; software: R.D.B. and V.V.; validation: G.D., R.D.B. and V.V.; formal analysis: V.V.; investigation: R.D.B. and V.V.; resources: R.D.B. and V.V.; data curation: V.V.; writing—original draft preparation: V.V.; writing—review and editing: G.D., R.D.B. and V.V.; visualization: V.V.; supervision: G.D. and R.D.B.; project administration: G.D.; funding acquisition: G.D. All authors have read and agreed to the published version of the manuscript.

Conflicts of interests

The authors declare no conflict of interest.

Nomenclature

Symbol	Description
N	Number of explanatory variables
T	Number of time periods / observations
$x_i^{(0)}(t)$	Original data of variable i at time t
$x_i^{(1)}(t)$	First-order accumulated data of variable i at time t
$z_i^{(1)}(t)$	Background value of variable i at time t
a	System development coefficient
b_i	Driver coefficient for variable i
b_{N+1}	Intercept term in the *GM(1,N)* model
$\varepsilon_i(t)$	Residual of variable i at time t
$S_i(t)$	Discretized residual state of variable i at time t
$e_{i;u}$	Unit vector for state u of variable i
$p_{u,v}^{(\beta,\alpha)}$	Transition probability from state u of variable β to state v of variable α
$\lambda_{\beta,\alpha}$	Weight of influence of variable β on α in MTD
$r_{\alpha;v}$	Representative value of state v for variable α
$\hat{x}_i^{(0)}(t)$	Predicted value of variable i at time t (before correction)
$\hat{\varepsilon}_\alpha$	Corrected residual for variable α
$\hat{\hat{x}}_i^{(0)}(t)$	Final prediction after residual correction
$P^{(\beta,\alpha)}$	One-step transition matrix from β to α
$(P^{(\beta,\alpha)})^k$	k-step transition matrix from β to α

Appendix A: *GM(1,N)* model

Suppose N is the number of the variables and the system characteristic factor's time sequence is

$$X_i^{(0)}(t) = \{x_i^{(0)}(1), x_i^{(0)}(2), \ldots, x_i^{(0)}(T)\}, \quad i = 1, 2, \ldots, T,$$

where t stands for the time and i for the variable.

Their first-order accumulated generating sequence is

$$x_i^{(1)}(t) = \sum_{h=1}^{t} x_i^{(0)}(h), \quad t = 1, 2, \ldots, T, \tag{4}$$

resulting in the following vector

$$X_i^{(1)}(t) = \{x_i^{(1)}(1), x_i^{(1)}(2), \ldots, x_i^{(1)}(T)\}, \quad i = 1, 2, \ldots, T.$$

Note that $x_i^{(0)}(1) = x_i^{(1)}(1)$.

Then, the background value $z_i^{(1)}(t)$ for the i variable at time t is defined as

$$z_i^{(1)}(t) = \frac{1}{2}x_i^{(1)}(t-1) + \frac{1}{2}x_i^{(1)}(t), \quad t = 2,3,\ldots,T.$$

The set of background values is stored in the following vector

$$Z_i^{(1)}(t) = \{z_i^{(1)}(2), z_i^{(1)}(2), \ldots, x_i^{(1)}(T)\}, \quad i = 1,2,\ldots,T.$$

Assuming we aim to forecast variable $i = 1$ based on the other $N-1$ variables, the conventional Grey model *GM(1,N)*'s first order difference equation is given by

$$x_1^{(0)}(t) + az_1^{(1)}(t) = b_2x_2^{(1)}(t) + b_3x_3^{(1)}(t) + \cdots + b_Nx_N^{(1)}(t), \tag{5}$$

where a is called the system development coefficient and b_i is called the driver coefficient. The differential equation, also called the whitenization equation, is

$$\frac{dx_1^{(1)}(t)}{dt} + ax_1^{(1)}(t) = \sum_{i=2}^{N} b_ix_i^{(1)}(t). \tag{6}$$

The parameter estimation for the GM(1,N) is performed as follows. The system of equations can be represented in matrix form as:

$$\hat{B} = \begin{pmatrix} a \\ b_2 \\ \vdots \\ b_N \end{pmatrix} = (X^TX)^{-1}X^TY, \tag{7}$$

$$X = \begin{pmatrix} -z_1^{(1)}(2) & x_2^{(1)}(2) & \cdots & x_N^{(1)}(2) \\ -z_1^{(1)}(3) & x_2^{(1)}(3) & \cdots & x_N^{(1)}(3) \\ \vdots & \vdots & \ddots & \vdots \\ -z_1^{(1)}(T) & x_2^{(1)}(T) & \cdots & x_N^{(1)}(T) \end{pmatrix}, \quad Y = \begin{pmatrix} x_1^{(0)}(2) \\ x_1^{(0)}(3) \\ \vdots \\ x_1^{(0)}(T) \end{pmatrix}.$$

In our article, we aim to generalize this model by adding an intercept term b_{N+1}. Therefore, we rewrite Equation (5) and Equation (6) as follows:

$$x_1^{(0)}(t) + az_1^{(1)}(t) = b_2x_2^{(1)}(t) + b_3x_3^{(1)}(t) + \cdots + b_Nx_N^{(1)}(t) + b_{N+1}.$$

$$\frac{dx_1^{(1)}(t)}{dt} + ax_1^{(1)}(t) = \sum_{i=1}^{N} b_ix_i^{(1)}(t) + b_{N+1}.$$

For the same reason, the previous matrices must also be updated

$$\hat{B} = \begin{pmatrix} a \\ b_2 \\ \vdots \\ b_N \\ b_{N+1} \end{pmatrix} = (X^T X)^{-1} X^T Y,$$

$$X = \begin{pmatrix} -z_1^{(1)}(2) & x_2^{(1)}(2) & \cdots & x_N^{(1)}(2) & 1 \\ -z_1^{(1)}(3) & x_2^{(1)}(3) & \cdots & x_N^{(1)}(3) & 1 \\ \vdots & \vdots & \ddots & \vdots & \vdots \\ -z_1^{(1)}(T) & x_2^{(1)}(T) & \cdots & x_N^{(1)}(T) & 1 \end{pmatrix}, \quad Y = \begin{pmatrix} x_1^{(0)}(2) \\ x_1^{(0)}(3) \\ \vdots \\ x_1^{(0)}(T) \end{pmatrix}.$$

The solution of the whitenization equation is

$$\hat{x}_1^{(1)}(t) = e^{-a(t\ -\ 1)} x_1^{(1)}(1) + e^{-at} \left[\int_1^t e^{as} \left(\sum_{i=2}^{N} b_i x_i^{(1)}(s) + b_{N+1} \right) ds \right].$$

When the variation in $X_i^{(1)}(t)$ is very small, assuming $\sum_{i=2}^{N} b_i x_i^{(1)}(t)$ as a constant [53], the time response equation is

$$\hat{x}_1^{(1)}(t) = e^{-a\cdot(t\ -\ 1)} \left[x_1^{(1)}(1) - \frac{1}{a} \left(\sum_{i=2}^{N} b_i x_i^{(1)}(t\ +\ 1) + b_{N+1} \right) \right] + \frac{1}{a} \left(\sum_{i=2}^{N} b_i x_i^{(1)}(t\ +\ 1) + b_{N+1} \right).$$

The estimated value is finally used to correct the forecast, completing the prediction update process, after which the simulated and predicted values of the original sequence can be obtained from the relation $\hat{x}^{(0)}(t) = \hat{x}^{(1)}(t) - \hat{x}^{(1)}(t-1)$.

Note that the entire procedure is repeated for each variable i in the system.

References

[1] Xu Y, Singh C. Adequacy and economy analysis of distribution systems integrated with electric energy storage and renewable energy resources. *IEEE Trans. Power Syst.* 2012, 27(4):2332–2341.

[2] Ghalehkhondabi I, Ardjmand E, Weckman GR, Young WA. An overview of energy demand forecasting methods published in 2005–2015. *Energy Syst.* 2017, 8:411–447.

[3] Liu Y, Roberts MC, Sioshansi R. A vector autoregression weather model for electricity supply and demand modeling. *J. Mod. Power Syst. Clean Energy* 2018, 6(4):763–776.

[4] Casula L, D'Amico G, Masala G, Petroni F. A multivariate model for hybrid wind–photovoltaic power production with energy portfolio optimization. *J. Energy Mark.* 2022, 15(3):1–29.

[5] Ediger VŞ, Akar S. ARIMA forecasting of primary energy demand by fuel in Turkey. *Energy Policy* 2007, 35(3):1701–1708.

[6] Chodakowska E, Nazarko J, Nazarko Ł, Rabayah HS, Abendeh RM, *et al.* Arima models in solar radiation forecasting in different geographic locations. *Energies* 2023, 16(13):5029.

[7] Hasanov FJ, Hunt LC, Mikayilov CI. Modeling and forecasting electricity demand in Azerbaijan using cointegration techniques. *Energies* 2016, 9(12):1045.

[8] Li S, Li R. Comparison of forecasting energy consumption in Shandong, China using the ARIMA model, GM model, and ARIMA-GM model. *Sustainability* 2017, 9(7):1181.

[9] Kalogirou SA. Applications of artificial neural-networks for energy systems. *Appl. Energy* 2000, 67(1–2):17–35.

[10] Lu C, Li S, Lu Z. Building energy prediction using artificial neural networks: a literature survey. *Energy Build.* 2022, 262:111718.

[11] Xu L, Hou L, Zhu Z, Li Y, Liu J, *et al.* Mid-term prediction of electrical energy consumption for crude oil pipelines using a hybrid algorithm of support vector machine and genetic algorithm. *Energy* 2021, 222:119955.

[12] Guermoui M, Gairaa K, Boland J, Arrif T. A novel hybrid model for solar radiation forecasting using support vector machine and bee colony optimization algorithm: review and case study. *J. Sol. Energy Eng.* 2021, 143(2):020801.

[13] Ali M, Prasad R, Xiang Y, Khan M, Farooque AA, *et al.* Variational mode decomposition based random forest model for solar radiation forecasting: new emerging machine learning technology. *Energy Rep.* 2021, 7:6700–6717.

[14] Fan G, Zhang L, Yu M, Hong W, Dong S. Applications of random forest in multivariable response surface for short-term load forecasting. *Int. J. Electr. Power Energy Syst.* 2022, 139:108073.

[15] Deng J. Control problems of grey system. *Syst. Control Lett.* 1982, 1:288–294.

[16] Liu S, Forrest JYL. *Grey systems: theory and applications*, 1st ed. Berlin: Springer, 2010. pp. 1–379.

[17] Tseng ML. Using linguistic preferences and grey relational analysis to evaluate the environmental knowledge management capacity. *Expert Syst. Appl.* 2010, 37(1):70–81.

[18] Raheem I, Mubarak NM, Karri RR, Manoj T, Ibrahim SM, *et al.* Forecasting of energy consumption by G20 countries using an adjacent accumulation grey model. *Sci. Rep.* 2022, 12(1):13417.

[19] Ma X, Lu H, Ma M, Wu L, Cai Y. Urban natural gas consumption forecasting by novel wavelet-kernelized grey system model. *Eng. Appl. Artif. Intell.* 2023, 119:105773.

[20] Golinska P, Kosacka M, Mierzwiak R, Werner-Lewandowska K. Grey decision making as a tool for the classification of the sustainability level of remanufacturing companies. *J. Cleaner Prod.* 2015, 105:28–40.

[21] Javanmardi E, Liu S. Exploring the human cognitive capacity in understanding systems: a grey systems theory perspective. *Found. Sci.* 2020, 25:803–825.

[22] Tao L, Liang A, Xie N, Liu S. Grey system theory in engineering: a bibliometrics and visualization analysis. *Grey Syst. Theory Appl.* 2022, 12(4):723–743.

[23] Comert G, Begashaw N, Huynh N. Improved grey system models for predicting traffic parameters. *Expert Syst. Appl.* 2021, 177:114972.

[24] Sahu AK, Datta S, Mahapatra SS. Supply chain performance benchmarking using grey-MOORA

approach: an empirical research. *Grey Syst. Theory Appl.* 2014, 4(1):24–55.

[25] Al-shanini A, Ahmad A, Khan F, Oladokun O, Mohd Nor SH. Alternative prediction models for data scarce environment. In *12th International Symposium on Process Systems Engineering and 25th European Symposium on Computer Aided Process Engineering*, Copenhagen, Denmark, May 31 to June 4, 2015, pp. 665–670.

[26] Liu C. Empirical analysis of the relationship between renewable energy consumption and economic growth based on the Grey Markov model. *J. Math.* 2022, 2022(1):5679696.

[27] Li Q, Dang Y, Wang Z. Analysis of the regional coordination development systems based on GRA and *GM (1, N). J. Grey Syst.* 2012, 24(1):95.

[28] Deng C, Zhang S, Deng J. Numerical mapping in DNA sequences and analysis of the genetic information by *GM (1, N). J. Grey Syst.* 2012, 24(3):217.

[29] Ren J, Gao S, Tan S, Dong L. Prediction of the yield of biohydrogen under scanty data conditions based on *GM (1, N). Int. J. Hydrogen Energy* 2013, 38(30):13198–13203.

[30] Deng J. Introduction to grey system theory. *J. Grey Syst.* 1989, 1(1):1–24.

[31] Tien T. The indirect measurement of tensile strength of material by the grey prediction model *GMC (1, N). Meas. Sci. Technol.* 2005, 16(6):1322.

[32] Tien T. A research on the grey prediction model *GM (1, N). Appl. Math. Comput.* 2012, 218(9):4903–4916.

[33] Deng J. *Gray decision and prediction*, 1st ed. Wuhan: Huazhong University of Science and Technology Press, 1986. pp. 1–200.

[34] Lu X, Luo X, Li H. The Grey Markov chain model for prediction of first frost and its utilization. *Chin. J. Agrometeorol.* 1997, 18(5).

[35] Qian J, Zhu X, Wu J, Pan G. Grey Markov model for predicting mine discharge. *J. China Coal Soc.* 2000, 25:71–75.

[36] Lee C, Lin CT, Chent LH. Accuracy analysis of the Grey Markov forecasting model. *J. Stat. Manage. Syst.* 2004, 7(3):567–580.

[37] He Y, Bao Y. Grey-Markov forecasting model and its application. *Syst. Eng. Theory Pract.* 1992, 9(4):59–63.

[38] Huang M, He Y, Cen H. Predictive analysis on electric-power supply and demand in China. *Renewable Energy* 2007, 32(7):1165–1174.

[39] D'Amico G, Karagrigoriou A, Vigna V. Forecasting the power generation mix in Italy based on Grey Markov models. *Energies* 2024, 17(9):2184.

[40] Morcous G, Lounis Z. Maintenance optimization of infrastructure networks using genetic algorithms. *Autom. Constr.* 2005, 14(1):129–142.

[41] Li GD, Yamaguchi D, Nagai M. A GM (1, 1)–Markov chain combined model with an application to predict the number of Chinese international airlines. *Technol. Forecasting Social Change* 2007, 74(8):1465–1481.

[42] Sun X, Sun W, Wang J, Zhang Y, Gao Y. Using a Grey–Markov model optimized by Cuckoo search algorithm to forecast the annual foreign tourist arrivals to China. *Tour. Manag.* 2016, 52:369–379.

[43] Li P, Li J. Exploration of the application of Grey-Markov models in the causality analysis of traffic accidents in roundabouts. *PLOS ONE* 2023, 18:1–21.

[44] Raftery AE. A model for high-order Markov chains. *J. R. Stat. Soc. Ser. B Stat. Methodol.* 1985, 47(3):528–539.

[45] Berchtold A, Raftery A. The mixture transition distribution model for high-order Markov chains and non-Gaussian time series. *Stat. Sci.* 2002, 17(3):328–356.

[46] Ching WK, Fung ES, Ng MK. A multivariate Markov chain model for categorical data sequences and its applications in demand predictions. *IMA J. Manage. Math.* 2002, 13(3):187–199.

[47] Ruoso AC, Bitencourt LC, Sudati LU, Klunk MA, Caetano NR. New parameters for the forest biomass waste ecofirewood manufacturing process optimization. *Periód. Tchê Quím.* 2019, 16(32):560–571.

[48] Álvarez-Arroyo C, Vergine S, D'Amico G, Escaño JM, Alvarado-Barrios L. Dynamic optimisation of unbalanced distribution network management by model predictive control with Markov reward processes. *Heliyon* 2024, 10(2):e24760.

[49] Hu Y, Jiang P, Chiu Y, Tsai J. A novel grey prediction model combining markov chain with functional-link net and its application to foreign tourist forecasting. *Information* 2017, 8(4):126.

[50] Zhanli M, Sun J. Application of Grey-Markov model in forecasting fire accidents. *Procedia Eng.* 2011, 11:314–318.

[51] D'Amico G, De Blasis R. A multivariate Markov chain stock model. *Scand. Actuarial J.* 2020, 2020(4):272–291.

[52] D'Amico G, De Blasis R, Petroni F. The mixture transition distribution approach to networks: evidence from stock markets. *Physica A* 2023, 632:129335.

[53] Li C, Li Y, Xing J. Multivariate grey prediction model application in civil aviation carbon emission based on fractional order accumulation and background value optimization. *Sustainability* 2023, 15(11):9127.